

Piezoelectric Properties of PVDF Modified 3-3 Type Cement-Based Piezoelectric Composites

Wei Liu (✉ lwnuc@163.com)

North University of China <https://orcid.org/0000-0002-6142-9754>

lehui zhang

North University of China

Yu Cao

North University of China

Jianhong Wang

North University of China

Peikang Bai

North University of China

Jinlong Yang

Tsinghua University

Research Article

Keywords: 3-3 type cement-based piezoelectric composites, Polyvinylidene fluoride, microstructure, electric properties, electromechanical properties

Posted Date: December 21st, 2020

DOI: <https://doi.org/10.21203/rs.3.rs-131867/v1>

License:   This work is licensed under a Creative Commons Attribution 4.0 International License.

[Read Full License](#)

Abstract

In this study, 3-3 type cement-based piezoelectric composites were prepared by casting Portland cement paste in porous lead zirconate titanate (PZT) ceramics, then the Polyvinylidene fluoride (PVDF) of N-Methylpyrrolidone (NMP) solvent with concentration of 50-200 mg/ml was utilized to modify the PZT-PC composites. The influence of PVDF concentration on the density, microstructure, dielectric, piezoelectric and electromechanical properties were investigated. The results indicate that the density of PZT-PC composites increased gradually with PVDF concentration for the increasing combined weight of PVDF with the composites. The introduction of PVDF has also contributed to the reduction of leakage current during the poling and testing process, which led to increased relative permittivity ϵ_r and longitudinal piezoelectric strain coefficient d_{33} , while the dielectric loss $\tan\delta$ and longitudinal piezoelectric voltage coefficient g_{33} demonstrated an opposite changing trend. Both the thickness electromechanical coupling coefficient K_t and planar electromechanical coupling coefficient K_p of the PZT-PC composites increased with PVDF concentration. The acoustic impedance (Z) of PVDF modified PZT-PC composites ranged from 6.89 to 7.65 MRays, making it suitable for applications in the health monitoring of civil engineering.

1. Introduction

With the modern development of civil engineering, the smart material and structure is being introduced. In a smart monitoring system, sensors and actuators are essential components for sensing and controlling purpose. Cement-based piezoelectric composites, by virtue of their excellent piezoelectric properties and good acoustic impedance compatibility with the civil engineering's main structural material-concrete, have been considered to be optimal candidate for smart materials in the field of civil engineering monitoring[1–5]. In previous research studies, 0–3, 1–3 and 2–2 type (the first number represents the connectivity of active piezoelectric phase and the second is that of passive cement phase) cement-based piezoelectric composites have been widely investigated[6–9].

Compared to 1–3 and 2–2 type composites, the study of 0–3 type composites has made great progress for the simplest fabrication procedure, which just mixes ceramic particles into the cement matrix by ball-milling method, and then the mixed materials are pressed into disks with the required size[10, 11]. Nonetheless, the 0–3 type piezoelectric composites still have difficulty in obtaining good piezoelectric properties due to the incomplete polarization of piezoelectric ceramic phase during the poling process. For one thing, the electric current could not fully act on the piezoelectric phase on account of being surrounded by the cement matrix, for another, the leakage current caused by the interface pore, the cement matrix pore and their inner water also exerts a negative impact on the degree of poling. Therefore, carbon nanotubes or carbon black are added as a third conductive phase to establish continuous electrical flux paths between the ceramic particles in the composites, and hence enable easier poling in such composites[12–15]. However, it is found that the dissipation energy in ferroelectric hysteresis loops and the dielectric loss in dielectric properties increase with the addition of conducting materials[16, 17].

Our group, by casting Portland cement paste in the 3–3 type porous PZT ceramics with continuous vibration, has successfully fabricated 3–3 type cement-based piezoelectric composites, where the porous PZT ceramics were produced by combining the ultrastable particle-stabilized ceramic foams and gelcasting method in previous research. Obviously, the connectivity of piezoelectric phase in composites has contributed to the degree of polarization effect for the continuous electric current flow, and thus the promotion of piezoelectric properties. But it is very hard for the cement paste to fill in the submicron pores of porous PZT ceramics, so the interface pores between PZT ceramics and cement matrix still exist with leakage current arising during the poling process. To solve this problem, polymer materials can be added to the composites. As is known to all, polyvinylidene fluoride (PVDF) is a type of semicrystalline polymer with pyroelectric and piezoelectric properties. Its low dielectric loss, low acoustic impedance and relatively high piezoelectric coefficients make it promising candidate for applications in ultrasonic transducer, sensor, and actuator[17–20]. It is meaningful to utilize PVDF as a third-phase filler to aid the poling of cement-based piezoelectric composites.

In the present work, we have prepared 3–3 type cement-based PZT composites by casting cement paste into the 3–3 type porous PZT ceramics, then the PVDF of N-Methylpyrrolidone (NMP) solvent with different concentrations were produced, and brushed on the surface of PZT-PC composites to fabricate the PVDF-modified 3–3 type cement-based piezoelectric composites. The effect of PVDF concentration on the microstructure, dielectric, piezoelectric and electromechanical properties were investigated.

2. Experimental Procedure

2.1 Materials

PZT-5H powders (BaoDing HongSheng Acoustics Electron Apparatus Co., Ltd, China) were employed in the experiment. For the preparation of porous PZT ceramics, the short-chain amphiphilic molecules to hydrophobize the ceramic particle surface were valeric acid ($C_5H_{10}O_2$). Acrylamide (AM, $C_2H_3CONH_2$) and *N, N'*-methylenebisacrylamide (MBAM, $(C_2H_3CONH)_2CH_2$) were selected as the organic monomers. Ammonium persulfate (APS, $(NH_4)_2S_2O_8$, 35 wt%) as an initiator and *N, N, N', N'*-tetramethylenediamine (TEMED) as a catalyst were employed for the gelation process. Portland 42.5 cement (Taiyuan Lionhead Cement Co. Ltd., China), polyvinylidene fluoride (PVDF) and N-Methylpyrrolidone (NMP) were adopted to fabricate the piezoelectric composites, respectively.

2.2 Fabrication procedure

The preparation procedure of 3–3 type porous PZT ceramics is basically the same as our previous research[21, 22]. Summarily, the suspension with valeric acid concentration of 70 mmol/L and solid loading of 15 vol% was prepared by ball-milling quantitative PZT powder and valeric acid solution in the premix solution (water: AM: MBAM = 85: 14.5: 0.5). Then the mechanical stirring was utilized to generate bubbles in the suspension, during which, the catalyst and initiator were added with the amounts of

0.5 vol% and 1 vol% to stimulate the polymerization. Finally, the green parts were dried and sintered at 1150 °C to obtain the 3–3 type porous PZT ceramics.

For the fabrication of cement-based piezoelectric composites, the Portland cement paste (water to cement ratio (by weight) = 0.35) was cast in the porous PZT ceramics with constant vibration, and subsequently cured in moisture (temperature 20 ± 1 °C, relative humidity $\geq 90\%$) for 28 days.

PVDF solution with concentration of 50, 100, 150 and 200 mg/ml were prepared by dissolving quantitative PVDF powder in NMP solvent at 80 °C under constant rate of stirring to form a homogeneous solution. Then the solution was brushed on both surfaces of the PZT-PC composites to produce the PVDF modified 3–3 type cement-based piezoelectric composites, and vacuum treatment was employed to facilitate the pore-filling process. This operation was repeated five times to ensure sufficient combination of PVDF with the cement-based piezoelectric composites.

2.3 Characterization

The density of PZT-PC composites were measured by using the water displacement method based on Archimedean principles (ASTM C-373). Phase characteristic of the composites were investigated by X-ray diffraction (D/MAX-2400, Rigaku, Japan) using Ni-filtered CuK radiation. The field emission scanning electron microscope (FE–SEM) (MERLIN VP Compact; Carl Zeiss, Jena, Germany) were used to observe the microstructure of the porous ceramics and composites. For dielectric testing, all samples were machined to be disc-shaped with 20 mm in diameter and 5 mm in thickness. Both surfaces of the samples were coated with low-temperature silver paint, then the poling process was carried out under a poling field of 4 kV/mm for 30 min in silicone oil bath at 100 °C. The electromechanical, piezoelectric and dielectric properties were measured using a quasi-static d_{33} -meter (ZJ-3A; Institute of Acoustics, Chinese Academy of Science, Beijing, China) and impedance analyzer (HP-4194A; Hewlett-Packard Development Company, CA). The polarization-electric field (P - E) hysteresis loops were characterized at 100 Hz by a Sawyer-Tower circuit (RT6000HVA, Radiant Technologies Inc., Albuquerque, NM).

3. Results And Discussion

3.1 Microstructure and Phase characteristics

Figure 1 shows the detailed pore morphology and interconnection of porous ceramics and cement-based piezoelectric composites. As can be seen in Fig. 1(a), macropores with an average size of approximately 226 μm were formed in the porous PZT ceramics, and interconnected structure of open-cells were resembled, which was helpful for the cement paste to fill into the inner parts of porous ceramics.

Figure 1(b) demonstrates the fracture surfaces of cement-based piezoelectric composites without being modified by PVDF yet, while the PZT ceramic particles were surrounded by the cement hydrated products such as calcium silicate hydrate (C-S-H) and calcium hydroxide ($\text{Ca}(\text{OH})_2$), the PZT-PC composites were formed with significant enhancement of strength. However, there still existed some pores with an average size of 5 μm in the hydrated cement and at the interface binding between PZT particles and hydrate

cement, which would generate leakage current during the poling process and deteriorate the polarization effect. The microstructure of PVDF-modified 3–3 type cement-based piezoelectric composites with 100 mg/ml of PVDF is shown in Fig. 1(c), it can be found that not only the PZT piezoelectric ceramic particles were embraced by hydrated cement matrix, the PVDF polymer also infiltrated into the inner domain of composites as a connecting third phase and occupied the pore space between PZT ceramics and hydration products of cement. The existence of PVDF phase succeeded in reducing the defects in the composites and contributed to the improvement of poling process.

Figure 2 shows the density of PVDF-modified cement-based piezoelectric composites with different concentration of PVDF solution. It can be observed that with the increase in the concentration of PVDF solution, the density of PZT-PC composites was in the range from 3.43 g/cm³ to 3.61 g/cm³, which means an increase of ~ 5% and more PVDF occupying the pore space of cement-based piezoelectric composites. This result also indicates that the density of composites varied and could be easily tailored in a range to possess excellent piezoelectric properties by adjusting the concentration of PVDF solution.

Figure 3(a) reveals X-ray diffraction patterns of PVDF-modified cement-based piezoelectric composites with different concentration of PVDF solution. It is noted that the characteristic peaks appearing in the XRD traces of all PZT-PC composites were attributed to PZT ceramics where the peaks resembled those of a PZT ceramic matching JCPDS file no. 33–0784. Besides that, the main crystal hydrated products of tricalcium silicates (3CaO.SiO₂ or C3S) in cement such as calcium hydroxide (Ca(OH)₂) and the amorphous glassy phase of calcium silicate hydrates (C-S-H) were detected, but they were not as dominant as those of PZT due to both the preferred orientation of PZT and the relatively greater quantity of PZT ceramics. Calcium carbonate (CaCO₃), the reaction product of CO₂ and Ca(OH)₂ due to the sample exposure to air, was also detected. More importantly, the characteristic peaks corresponding to 2θ values around 18.37° and 19.93° revealed the existence of α and γ phase of PVDF. In general, the amplified diffraction peaks can be used to characterize the phase variation of PVDF modified cement-based piezoelectric composites. Therefore, the correspondingly amplified XRD patterns in the 2θ range of 17–21° are presented in Fig. 3(b). With increasing concentration of PVDF solution, the intensity of diffraction peaks nearby 18.37° and 19.93° increased gradually, which implies the increasing combined quantity of PVDF with the PZT-PC composites and is constant with the variation trends of density in Fig. 2.

3.2 Dielectric and piezoelectric properties

Figure 4 shows the relative permittivity (ϵ_r) of the PVDF-modified cement-based piezoelectric composites in the range of 100 Hz-2 MHz. As expected, the relative permittivity of all PVDF-modified cement-based piezoelectric composites decreased with increasing frequency and demonstrated ordinary ferroelectric property, it could be explained as follows: the dipole relaxation connected with domain walls motion of the ionic particles have made it hard for the electron hopping to follow the alternative field, for another, the inhomogeneities of PZT-PC composites gave rise to a frequency dependence of conductivity for the accumulating charge carries at the boundaries of less conducting regions, which led to the interfacial

polarization and the frequency shift of dipole lagging behind the electric field[23]. As far as to the effect of PVDF concentration on the relative permittivity, it is noted that the ϵ_r increased remarkably with the increasing concentration of PVDF solution, and the ϵ_r values at a frequency of 1 KHz were in the range from 360 to 406. It could be attributed to the infiltration of PVDF into the micron-sized pore space, the substitution of PVDF for air-filler pores has reduced the leakage current chiefly caused by the interface pore and cement matrix pore, and was in favor of high capacitance and the corresponding relative permittivity of PZT-PC composites[24].

The effect of PVDF concentration on the dielectric loss ($\tan\delta$) of PVDF-modified cement-based piezoelectric composites is shown in Fig. 5. The dielectric loss factor demonstrated a peaking behavior for all PZT-PC composites, which could be attributed to the dielectric relaxation phenomenon for many ferroelectrics. Moreover, owing to the insulating effect of the PVDF phase, the $\tan\delta$ values at a frequency of 1 KHz decreased from 0.04 to 0.02 with the increasing PVDF concentration.

Figure 6 shows the correlations of longitudinal piezoelectric strain coefficient (d_{33}) and longitudinal piezoelectric voltage coefficient (g_{33}) with concentration of PVDF solution. The d_{33} values of PZT-PC composites increased almost linearly from 270 to 289 $\mu\text{C}/\text{N}$ in the PVDF concentration range of 0-200 mg/ml. As is known, when the external electric field acts on the PZT-PC composites during the poling process, the weakly conducting ions (such as Ca^{2+} , OH^- and Al^{3+}) in cement phase tend to generate depolarization and make a shielding electric field to weaken the effect of external electric field[25]. Furthermore, the effect of leakage current that arises from micropores in the PZT-PC composites should not be neglected. Under the combined action of the two factors, the degree of poling process was brought down and the d_{33} values were reduced. When the PVDF phase was combined with the PZT-PC composites, it acted as an insulator with optimum effect and less conducting path connecting the porosity or conducting ion in the system, which resulted in greater electrical current flow to PZT phase and increasing values of d_{33} . The g_{33} value is defined as the ratio of d_{33} to $\epsilon_r \cdot \epsilon_0$, so the change in the g_{33} value depends on both the d_{33} and ϵ_r values. When the PVDF concentration ranged from 0 to 150 mg/ml, the g_{33} value decreased from 84.7 to 80.7 $\text{mV}\cdot\text{m}/\text{N}$, and then increased when the PVDF concentration went higher. It is believed that the descending trend of g_{33} values upon increasing the PVDF concentration to 150 mg/ml was mainly due to the faster increasing trend of ϵ_r than that of d_{33} . When exceeding the PVDF concentration of 150 mg/ml, the d_{33} value increased at a more rapid rate than ϵ_r , so the g_{33} value increased appropriately.

The ferroelectric hysteresis (P - E) loops were characterized to investigate the effect of PVDF concentration on the piezoelectric properties of PZT-PC composites. From Fig. 7, it is shown that all specimens exhibited typical P - E hysteresis loops at room temperature. The addition of PVDF exerted a significant influence on the remanent polarization P_r and coercive field E_c . With increasing the concentration of PVDF solution, the remanent polarization P_r and coercive field E_c increased. When the PVDF concentration increased from 0 to 200 mg/ml, the remanent polarization P_r increased from 1.05 to 5.91 $\mu\text{C}/\text{cm}^2$, and

the coercive field E_c increased from 1.29 to 6.01 kV/mm. Obviously, the leakage current caused by defects in the composites promoted the hysteresis loop to be less developed during the poling process and degraded the ferroelectric properties. Therefore, both the remnant polarization (P_r) and the longitudinal piezoelectric strain coefficient (d_{33}) of the 3–3 type cement-based piezoelectric composites could be improved as a function of PVDF modification. It should also be noticed that when the PVDF concentration was between 0 and 100 mg/ml, there was an obvious gap at the direction of the negative remanent polarization, which is still deduced to be caused by the leakage current. When the PVDF concentration increased to 150 mg/ml, the infiltration of PVDF into the pores reduced the leakage current and prevented the distortion of the hysteresis loops[26].

3.3 Electromechanical and acoustic properties

Figure 8 shows the impedance magnitude of the PZT-PC composites with different PVDF concentration. It can be seen that the impedance of the composites increased with PVDF concentration for the insulating property of PVDF phase. Meanwhile, there also appear some resonance peaks in all curves, which means that the PZT-PC composites possessed an electromechanical coupling behavior from the piezoelectric effect and inverse piezoelectric effect. The planar resonance peak of the composites was at the frequency zones between 50 kHz and 80 kHz, while the thickness resonance peak appeared around 200 kHz. With the increase of PVDF concentration, both the series resonance frequency and the parallel resonance frequency decreased accordingly, which resulted in the change of electromechanical coupling property.

In this study, the thickness electromechanical coupling coefficient K_t of the PVDF-modified cement-based piezoelectric composites were calculated from the impedance measurements according to the following formula[25]:

$$K_t^2 = \frac{\pi}{2} \cdot \frac{f_s}{f_p} \cdot \tan\left(\frac{\pi}{2} \cdot \frac{f_p - f_s}{f_p}\right) \quad (1)$$

where f_s and f_p are the series resonant frequency and the parallel resonant frequency, respectively, which can be replaced by the frequencies at the minimum and maximum impedances (f_m and f_n) in the fundamental resonant region of impedance spectrum. The planar electromechanical coupling coefficient K_p can approximately be evaluated using the curve of K_p versus $\Delta f/f_s$.

The acoustic impedance (Z) of the composites can be obtained by the following equation:

$$Z = 2 \cdot \rho_c \cdot d \cdot f_p \quad (2)$$

where d and ρ_c are the thickness and density of the composites respectively.

The electromechanical coupling coefficients of the PZT-PC composites with different PVDF concentration are summarized in Table I. It is observed that the thickness electromechanical coupling coefficient K_t increased from 30.83–42.02%, and the planar electromechanical coupling coefficient K_p increased from 22.53–32.25% with the combination of PVDF phase, which indicated higher resolution factor and thickness electromechanical transformation ability for the PVDF-modified cement-based piezoelectric composites to be used as the transducer. The acoustic impedance (Z) of PZT-PC composites decreased from 7.65 to 6.89 MRayls with the increasing PVDF concentration for the gradual introduction of the PVDF phase. The lower value of Z was close to that of concrete structures ($\sim 6.9 \sim 11.23$ MRayls), which is beneficial in improving acoustic matching and helpful for application in civil engineering.

4. Conclusion

In this work, PVDF modified 3–3 type cement-based piezoelectric composites were fabricated by filling the pores of 3–3 type PZT-PC composites with PVDF solution, while the PZT-PC composites were produced through casting cement paste into the 3–3 type porous PZT ceramics. The PVDF phase acted as a third phase in the PZT-PC composites and led to an increased density due to PVDF filling of the pores in the PZT-PC composites. As for the dielectric and piezoelectric properties of PVDF modified cement-based piezoelectric composites, the value of ϵ_r and d_{33} increased with the increasing PVDF concentration, while $\tan\delta$ and g_{33} exerted an opposite changing trend due to the reduction of leakage current by introducing PVDF phase. With increasing the PVDF concentration, both the thickness electromechanical coupling coefficient K_t and planar electromechanical coupling coefficient K_p of the PZT-PC composites increased accordingly. The acoustic impedance (Z) of PVDF modified PZT-PC composites ranged from 6.89 to 7.65 MRayls, remaining close to that of concrete structures.

Declarations

Acknowledgements

Our research work presented in this article is supported by National Natural Science Foundation of China (Grant nos. 51572140), Natural Science Foundation of Shanxi Province (No. 201901D111168), and Key Research and Development (R&D) Projects of Shanxi Province (Grant No. 201803D121037). The authors are grateful for these grants.

References

1. Santos JA, Sanches AO, Akasaki JL, Tashima MM, Longo E, Malmonge JA, Influence of PZT insertion on Portland cement curing process and piezoelectric properties of 0–3 cement-based composites by impedance spectroscopy, *Construction and Building Materials*, 238 (2020)
2. Pan HH, Wang C-K, Tia M, Su Y-M, Influence of water-to-cement ratio on piezoelectric properties of cement-based composites containing PZT particles, *Construction and Building Materials*, 239 (2020)

3. Sanches AO, Teixeira GF, Zaghete MA, Longo E, Malmonge JA, Silva MJ, Sakamoto WK, Influence of polymer insertion on the dielectric, piezoelectric and acoustic properties of 1-0-3 polyurethane/cement-based piezo composite, *Materials Research Bulletin*, 119 (2019)
4. Potong R, Rianyoi R, Ngamjarrojana A, Chaipanich A (2017) Microstructure and performance of 1–3 connectivity environmental friendly lead-free BNBK-Portland cement composites. *Mater Res Bull* 90:59–65
5. Jaitanong N, Chaipanich A, Tunkasiri T (2008) Properties 0–3 PZT-Portland cement composites. *Ceram Int* 34:793–795
6. Zhang Y, Liu Z, Zhang W (2019) Improved output voltage of 0–3 cementitious piezoelectric composites with basalt fibers. *Ceram Int* 45:6577–6580
7. Zhang F, Feng P, Wang T, Chen J, Mechanical-electric response characteristics of 1–3 cement based piezoelectric composite under impact loading, *Construction and Building Materials*, 228 (2019)
8. Zhang T, Liao Y, Zhang K, Chen J, Theoretical Analysis of the Dynamic Properties of a 2–2 Cement-Based Piezoelectric Dual-Layer Stacked Sensor under Impact Load, *Sensors (Basel, Switzerland)*, 17 (2017)
9. Xu D, Xin C, Banerjee S, Lei W, Huang S, Dielectric, piezoelectric and damping properties of novel 2–2 piezoelectric composites, *Smart Materials and Structures*, 24 (2015)
10. Potong R, Rianyoi R, Ngamjarrojana A, Yimnirun R, Guo R, Bhalla AS, Chaipanich A (2017) Thermal expansion behaviors of 0–3 connectivity lead-free barium zirconate titanate-Portland cement composites. *Ceram Int* 43:S129–S135
11. Pan HH, Lin DH, Yang RH (2016) High piezoelectric and dielectric properties of 0–3 PZT/cement composites by temperature treatment. *Cement Concr Compos* 72:1–8
12. Zhao P, Wang S, Kadlec A, Li Z, Wang X (2016) Properties of cement sand-based piezoelectric composites with carbon nanotubes modification. *Ceram Int* 42:15030–15034
13. Potong R, Rianyoi R, Ngamjarrojana A, Chaipanich A (2017) Influence of carbon nanotubes on the performance of bismuth sodium titanate-bismuth potassium titanate-barium titanate ceramic/cement composites. *Ceram Int* 43:S75–S78
14. Gong H, Zhang Y, Che S (2010) Influence of Carbon Black on Properties of PZT-Cement Piezoelectric Composites. *J Compos Mater* 44:2747–2757
15. Huang S, Li X, Liu F, Chang J, Xu D, Cheng X (2009) Effect of carbon black on properties of 0–3 piezoelectric ceramic/cement composites. *Curr Appl Phys* 9:1191–1194
16. Wittinanon T, Rianyoi R, Chaipanich A (2020) Effect of polyvinylidene fluoride on the fracture microstructure characteristics and piezoelectric and mechanical properties of 0–3 barium zirconate titanate ceramic-cement composites. *J Eur Ceram Soc* 40:4886–4893
17. Wittinanon T, Rianyoi R, Ngamjarrojana A, Chaipanich A, Effect of polyvinylidene fluoride on the acoustic impedance matching, poling enhancement and piezoelectric properties of 0–3 smart lead-free piezoelectric Portland cement composites, *Journal of Electroceramics*, (2020)

18. Jaitanong N, Narksitipan S, Chaipanich A (2017) Fabrication and electrical properties of PC-PNZT-PVDF-GO composites. *Integrated Ferroelectrics* 183:176–181
19. Jain A, Prashanth KJ, Sharma AK, Jain A, Rashmi PN (2015) Dielectric and piezoelectric properties of PVDF/PZT composites: A review. *Polym Eng Sci* 55:1589–1616
20. Shu L, Liang R, Rao Z, Fei L, Ke S, Wang Y (2019) Flexoelectric materials and their related applications: A focused review. *Journal of Advanced Ceramics* 8:153–173
21. Liu W, Xu J, Wang Y, Xu H, Xi X, Yang J (2013) Processing and Properties of porous PZT ceramics from particle-stabilized foams via gel casting. *J Am Ceram Soc* 96:1827–1831
22. Liu W, Du L, Wang Y, Yang J, Xu H (2013) Effects of foam composition on the microstructure and piezoelectric properties of macroporous PZT ceramics from ultrastable particle-stabilized foams. *Ceram Int* 39:8781–8787
23. Jaitanong N, Yimnirun R, Chaipanich A (2009) Effect of Uniaxial Stress on Dielectric Properties of 0–3 PZT-Portland Cement Composite. *Ferroelectrics* 384:174–181
24. Rianyo R, Potong R, Ngamjarrojana A, Chaipanich A (2018) Poling effects and piezoelectric properties of PVDF-modified 0–3 connectivity cement-based/lead-free $0.94(\text{Bi}_{0.5}\text{Na}_{0.5})\text{TiO}_3$ - 0.06BaTiO_3 piezoelectric ceramic composites. *Journal of Materials Science* 53:345–355
25. Huang S, Ye Z, Hu Y, Chang J, Lu L, Cheng X (2007) Effect of forming pressures on electric properties of piezoelectric ceramic/sulphoaluminate cement composites. *Composites Science Technology* 67:135–139
26. Xin C, Huang S, Jun C, Li Z, Piezoelectric, dielectric, and ferroelectric properties of 0–3 ceramic/cement composites, *Journal of Applied Physics*, 101 (2007)

Tables

Table I The electromechanical and acoustic properties of the PZT-PC composites with different concentration of PVDF solution.

Concentration of PVDF solution (mg/ml)	$K_t/\%$	$K_p/\%$	Z/MRayls
0	30.83	22.53	7.65
50	32.79	25.93	7.49
100	35.57	28.08	7.43
150	40.24	31.37	7.28
200	42.02	32.25	6.89

Figures

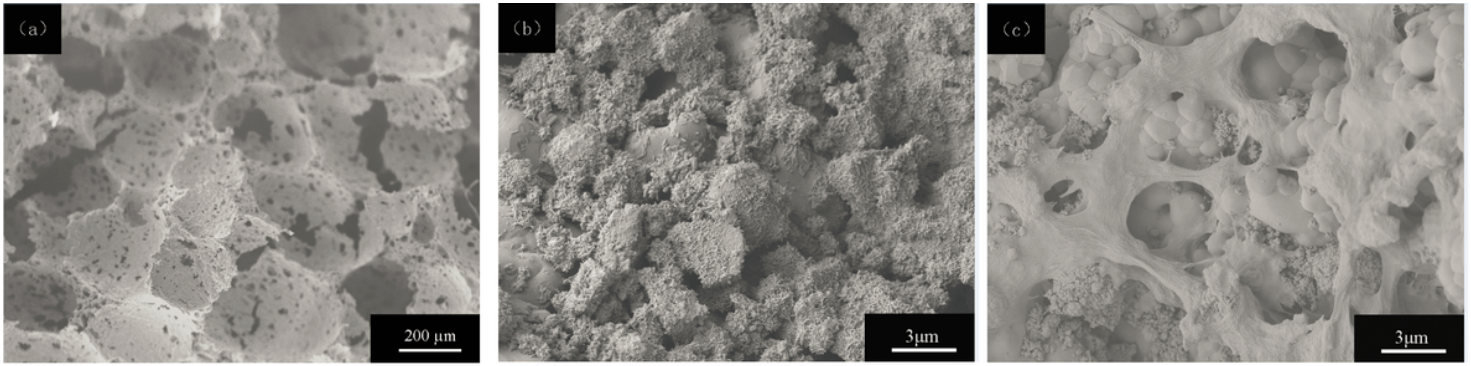


Figure 1

Scanning electron micrographs of (a) porous PZT ceramics, (b) cement-based piezoelectric composites and (c) PVDF modified cement-based piezoelectric composites with concentration of 10 mg/ml.

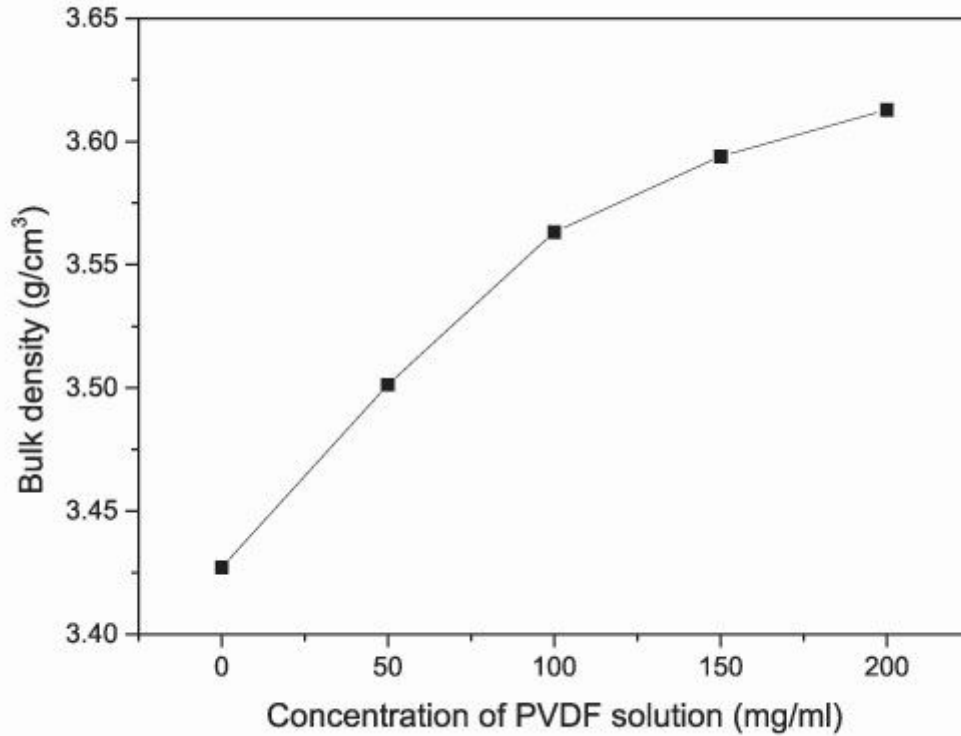


Figure 2

Variation in density of PZT-PC composites with PVDF concentration.

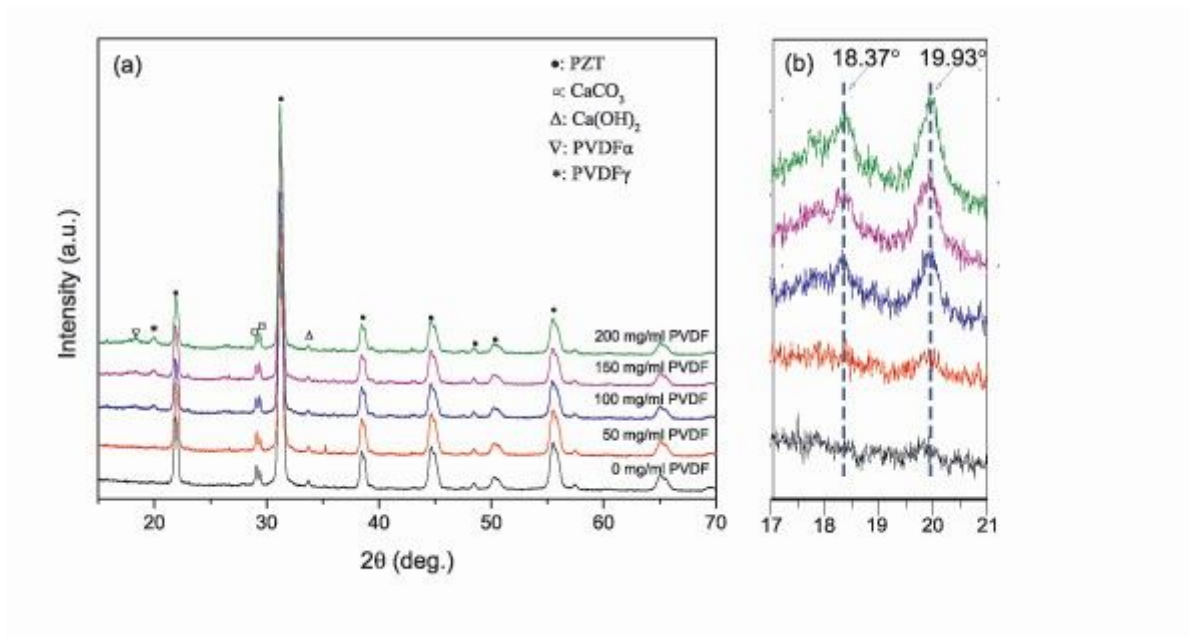


Figure 3

XRD patterns of PVDF modified cement-based piezoelectric composites with (a) $2\theta=15^\circ-70^\circ$, (b) $2\theta=17^\circ-21^\circ$.

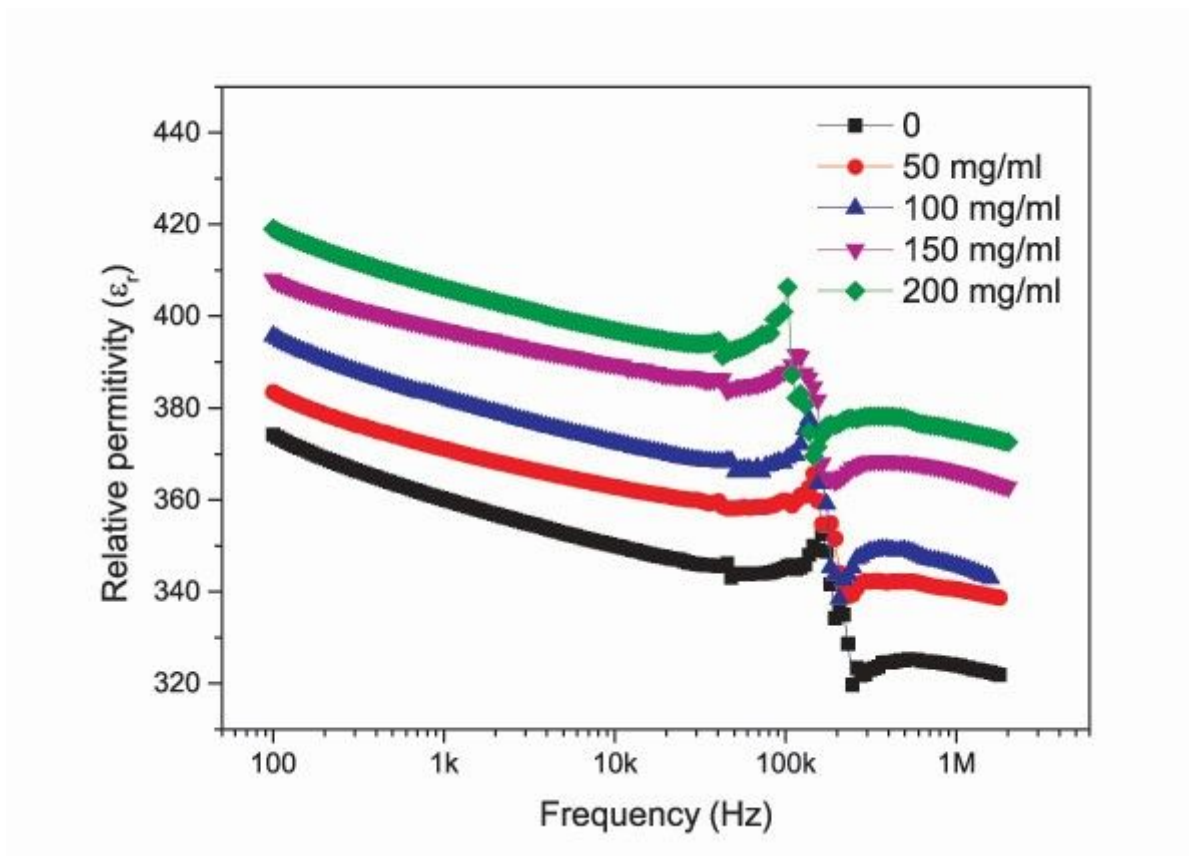


Figure 4

Variation of relative permittivity with frequency for PZT-PC composites modified with different concentration of PVDF solution.

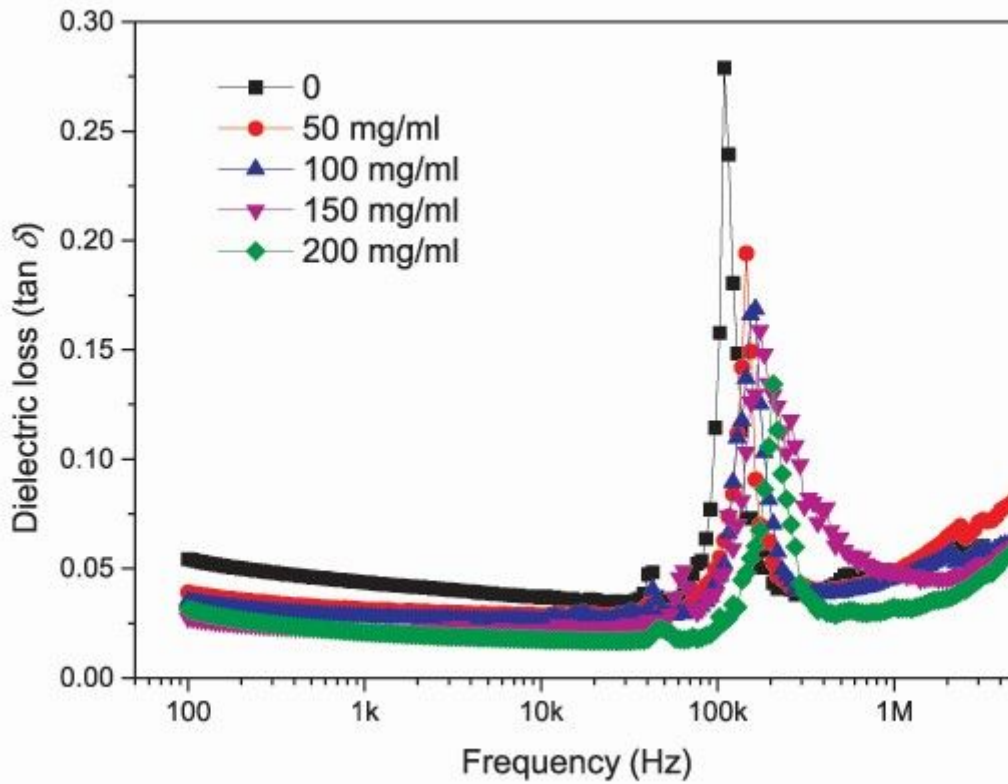


Figure 5

Variation of dielectric loss with frequency for PZT-PC composites modified with different concentration of PVDF solution.

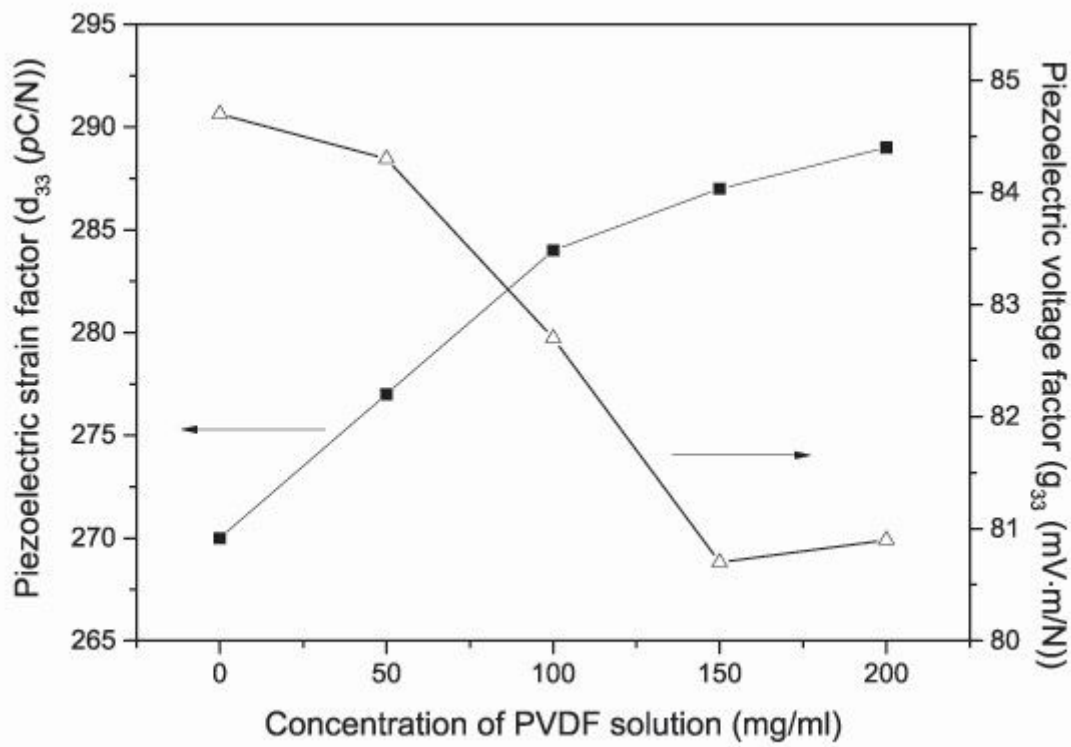


Figure 6

Longitudinal piezoelectric coefficient (d_{33}) and piezoelectric voltage coefficient (g_{33}) values of PZT-PC composites modified with different concentration of PVDF solution.

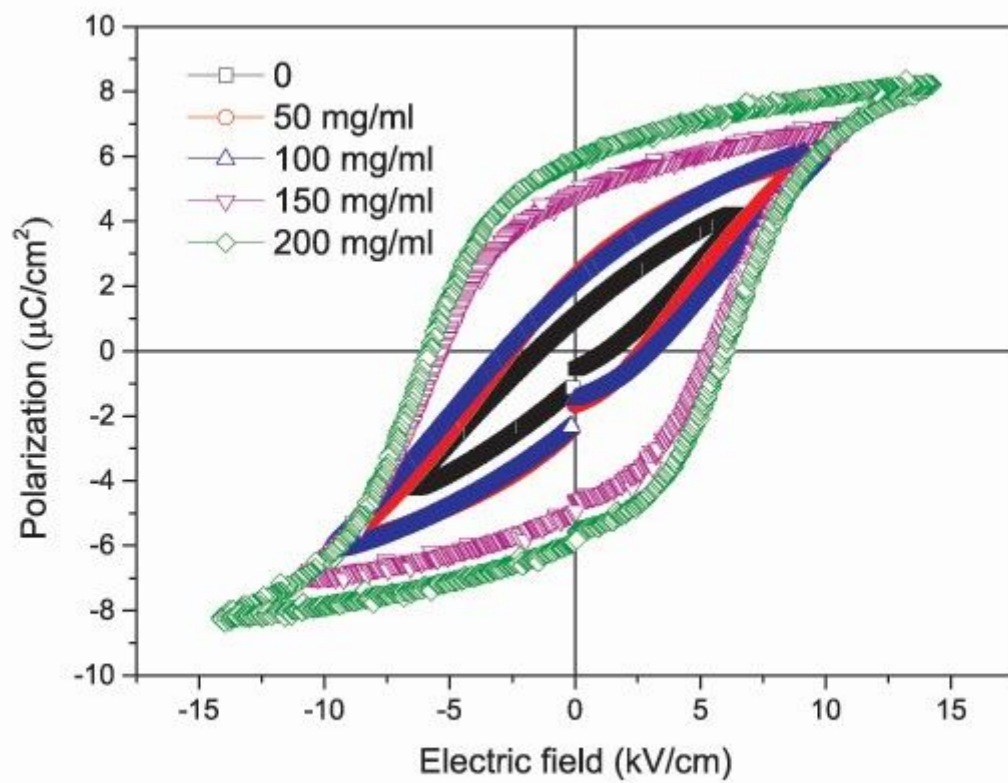


Figure 7

P-E hysteresis loops of PZT-PC composites vs concentration of PVDF solution.

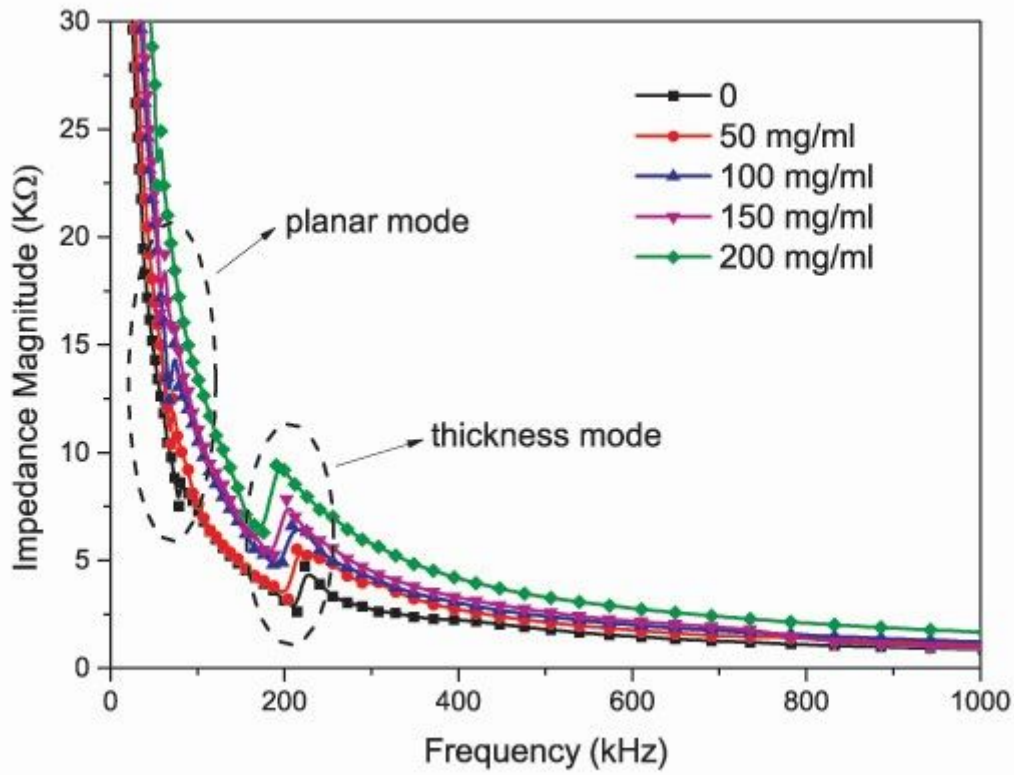


Figure 8

Impedance spectra of the PZT-PC composites with different concentration of PVDF solution.